Electronic Supplementary Information

Vapor-assisted self-conversion of basic carbonates in metal-organic frameworks

Miaomiao Jia, Jingyi Su, Pengcheng Su, Wanbin Li*

Guangdong Key Laboratory of Environmental Pollution and Health, School of Environment,

Jinan University, Guangzhou 511443, P.R. China

E-mail: gandeylin@126.com

This file includes:

Supplementary Figures S1 to S14

Supplementary Tables S1 and S8

Supplementary References 1 to 35

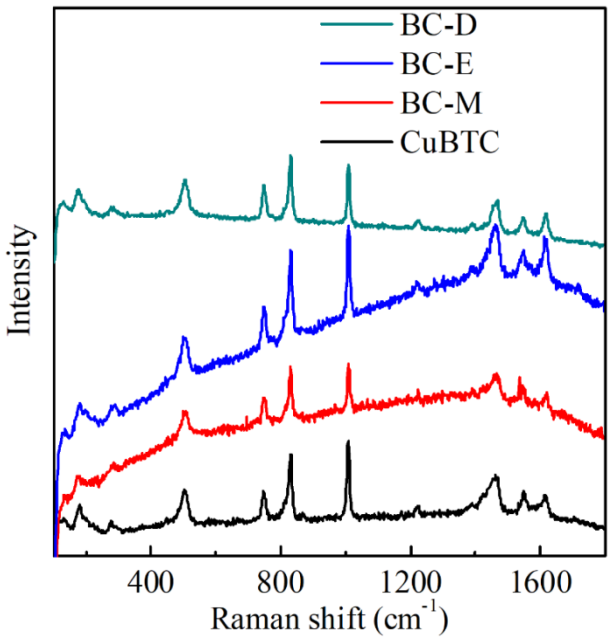

Fig. S1 Raman spectra of CuBTC and BC-CuBTC.

In the Raman spectra of the CuBTC and BC-CuBTC materials, the bands with peaks at 1460 and 1544 cm^{-1} were corresponded to O-C-O symmetric and asymmetric. The peak intensity of Cu-O_w at 277 cm^{-1} and Cu-O at 501 cm^{-1} in BC-CuBTC-M, BC-CuBTC-E, and BC-CuBTC-D showed some decrease compared with that of CuBTC[1]. The C-N peak belonging to DMF also exists at 866 cm^{-1} for CuBTC and BC-CuBTC materials. This indicates that solvent vapor-assisted thermal treatment cannot remove guest molecules in CuBTC.

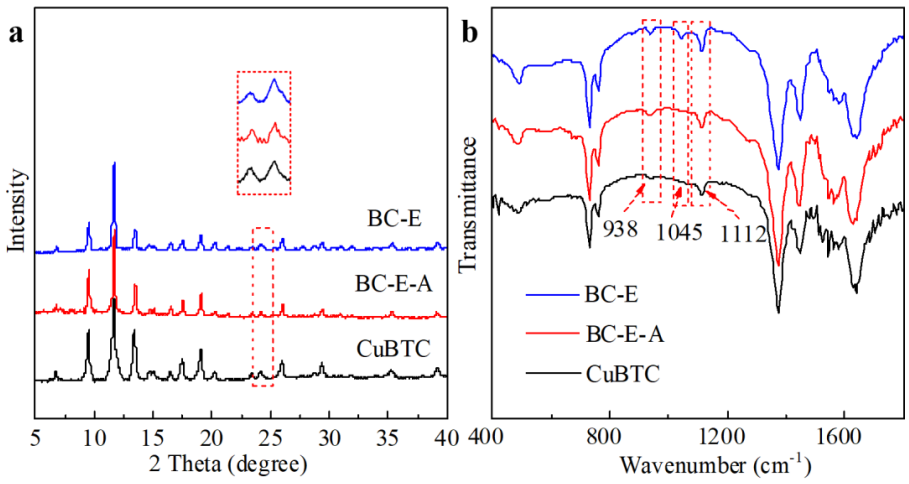

Fig. S2 (a) PXRD patterns and (b) FTIR spectra of CuBTC, BC-CuBTC-E-A, and BC-CuBTC-E.

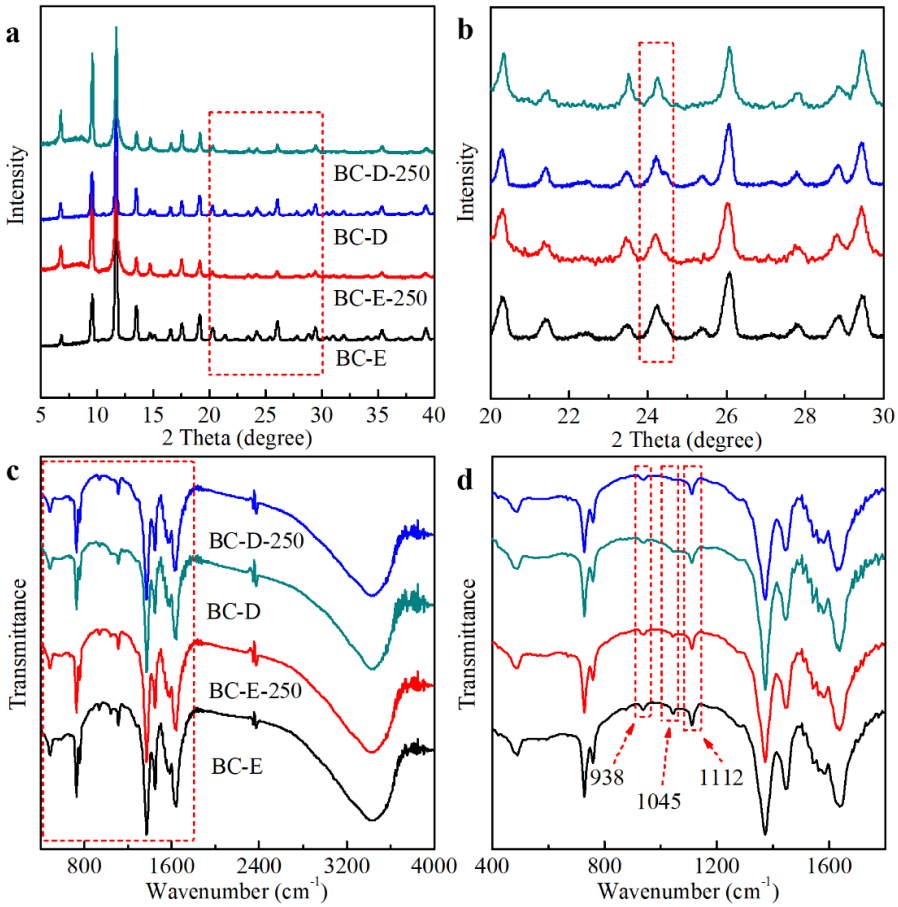

Fig. S3 (a,b) PXRD patterns and (c,d) FTIR spectra of BC-CuBTC-E, BC-CuBTC-E-250, BC-CuBTC-D, and BC-CuBTC-D-250.

The BC-CuBTC-E-250 and BC-CuBTC-D-250 materials were prepared by thermal treating BC-CuBTC-E and BC-CuBTC-D in vacuum at 250 ^{o}C for 8 h.

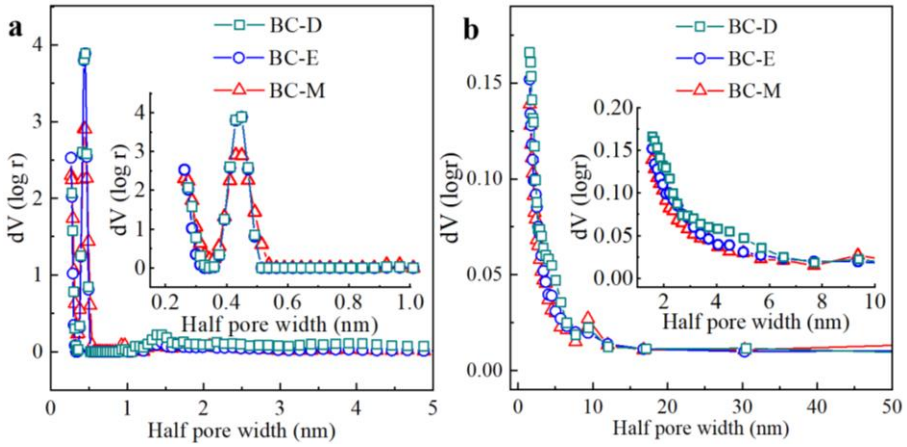

Fig. S4 Pore width distributions of BC-CuBTC from (a) density functional theory (DFT) method and (b) Barrett-Joyner-Halenda (BJH) method.

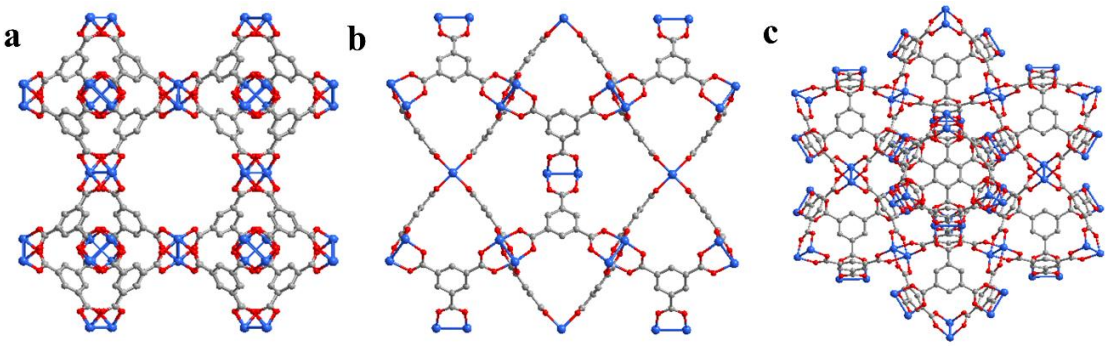

Fig. S5 CuBTC structure viewed at (a) {100}, (b) {110}, and (c) {111} facets.

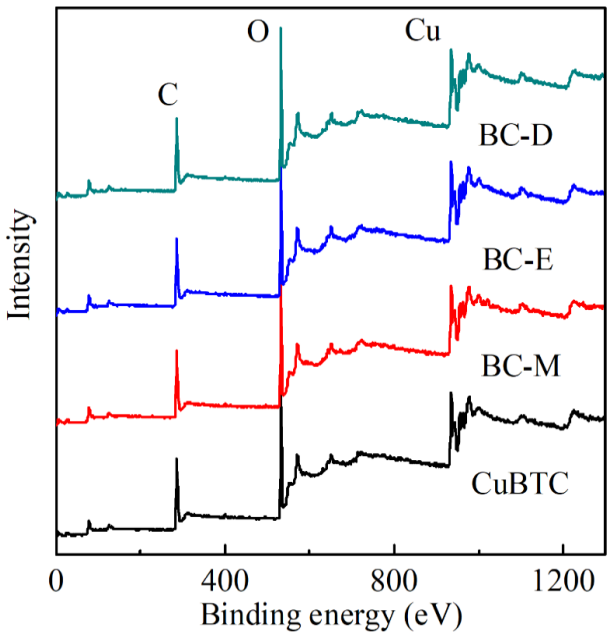

Fig. S6 XPS spectra of CuBTC, BC-CuBTC-M, BC-CuBTC-E, and BC-CuBTC-D.

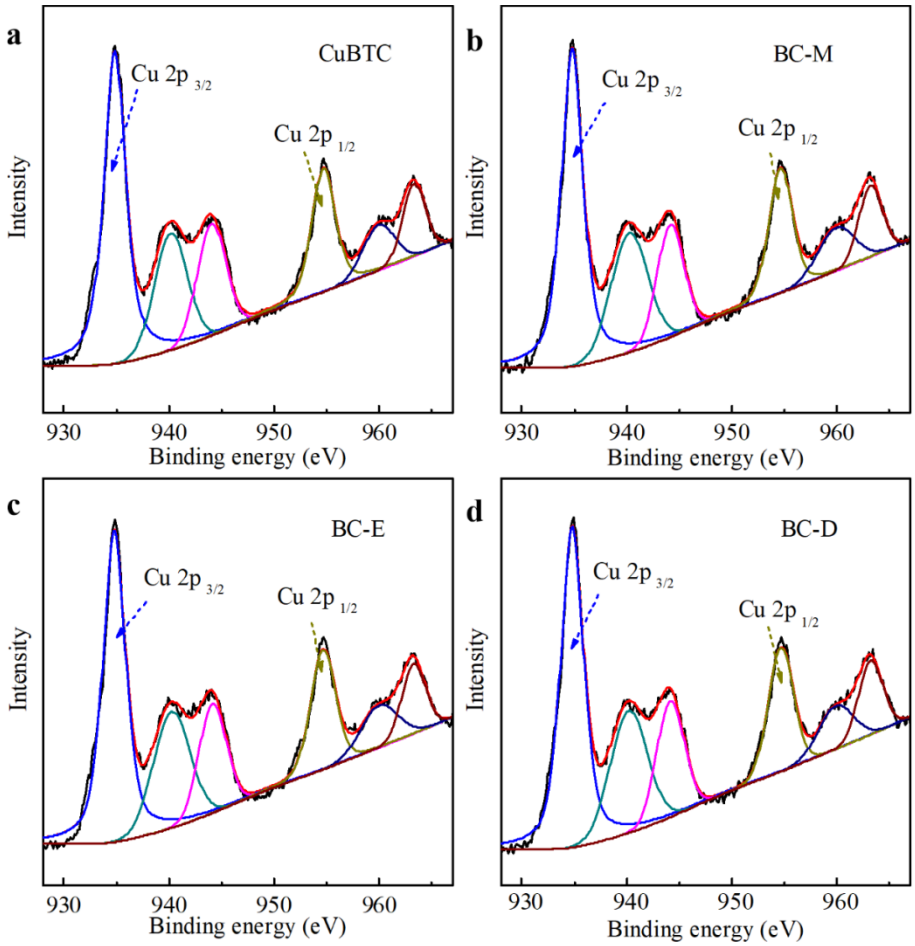

Fig. S7 (a) Cu 2p XPS profiles of (a) CuBTC, (b) BC-CuBTC-M, (c) BC-CuBTC-E, and (d) BC-CuBTC-D.

The high-resolution Cu 2p spectra showed that all samples had two main characteristic peaks of Cu 2p 3/2 at 935.0 eV and Cu 2p 1/2 at 954.9 eV, and four shake-up satellite peaks in the range of 930–965 eV. It could be confirmed that all Cu centers in CuBTC and BC-CuBTC existed in state of +2 valence.[2,3]

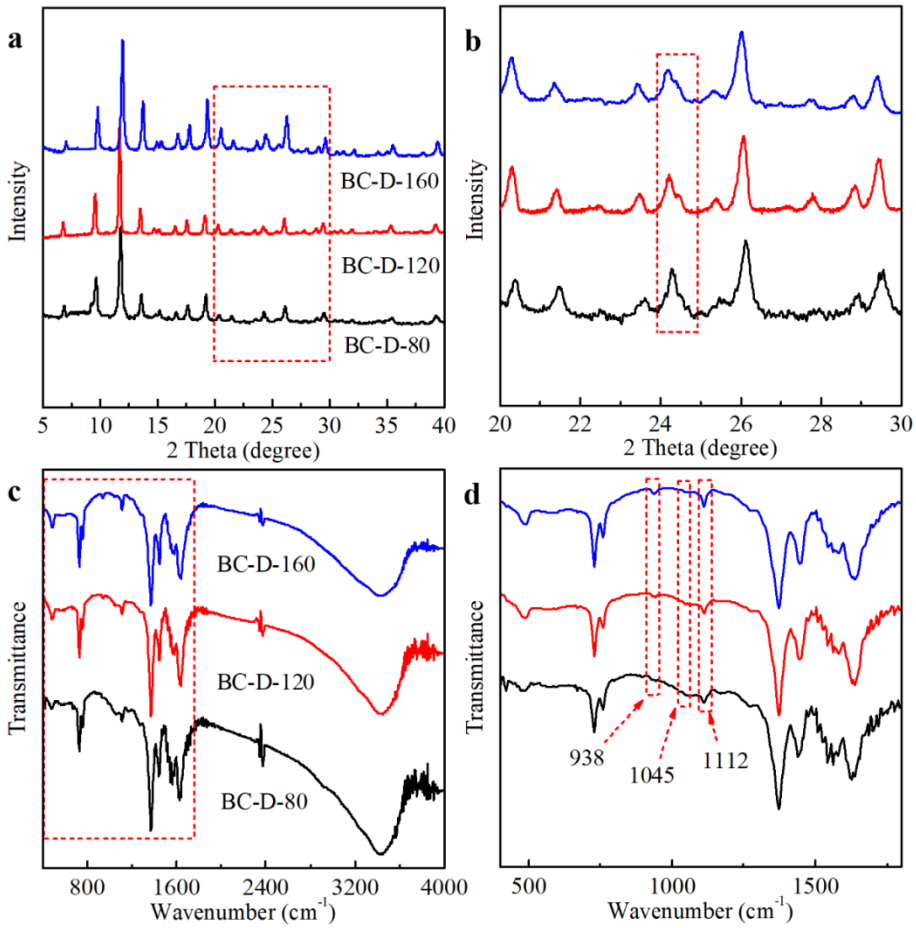

Fig. S8 (a,b) PXRD patterns and (c,d) FTIR spectra of BC-CuBTC-D-80, BC-CuBTC-D-120, and BC-CuBTC-D-160. The BC-CuBTC-D-80 and BC-CuBTC-D-160 were prepared with DMF solvent at 80 and 160 ^{o}C, respectively.

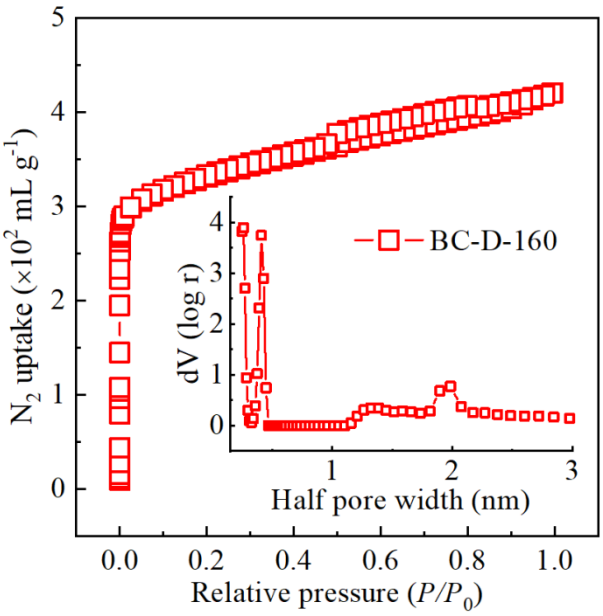

Fig. S9 N_2 adsorption-desorption isotherms and pore width distribution of BC-CuBTC-160.

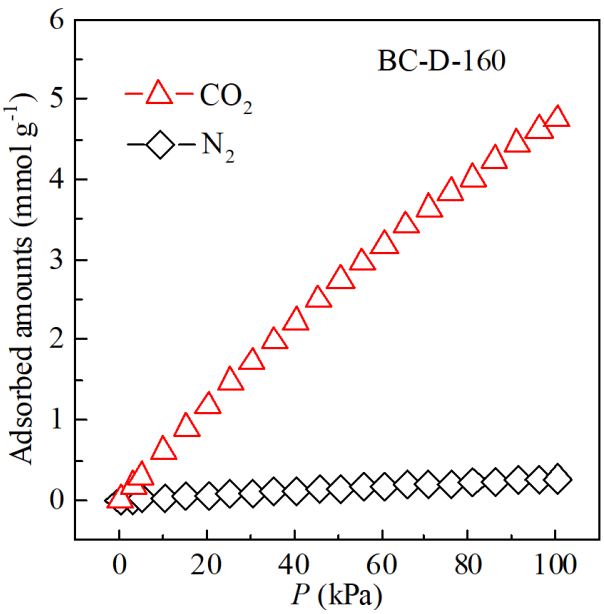

Fig. S10 CO_2 and N_2 adsorption isotherms of BC-CuBTC-D-160.

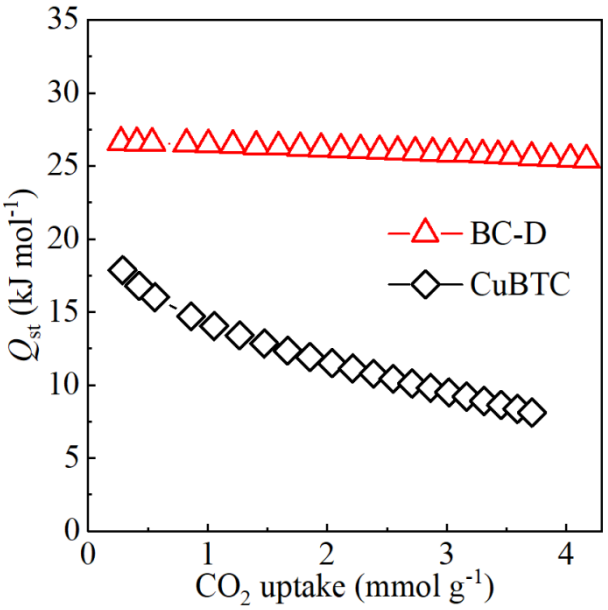

Fig. S11 Isosteric heat of adsorption (Q_{st}) for CO_2 of CuBTC and BC-CuBTC-D versus CO_2 uptake.

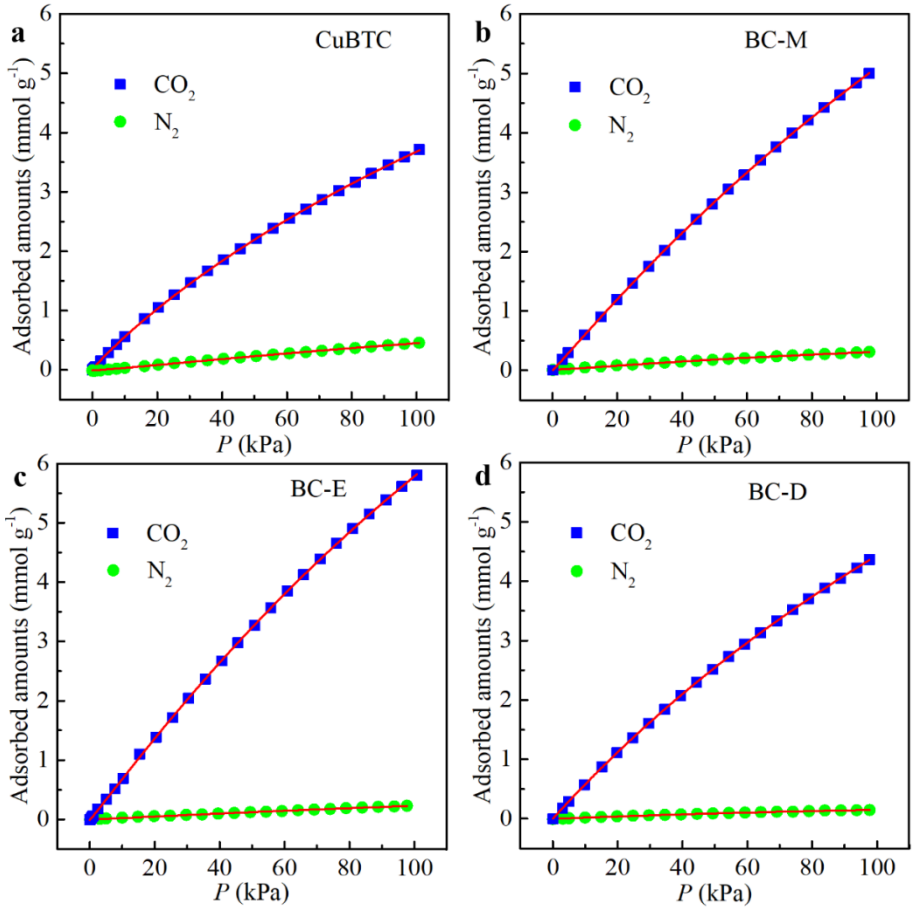

Fig. S12 CO_2 and N_2 adsorption isotherms of (a) CuBTC, (b) BC-CuBTC-M, (c) BC-CuBTC-E, and (d) BC-CuBTC-D. The isotherms were fitted by lines from single-site Langmuir-Freundlich equation.

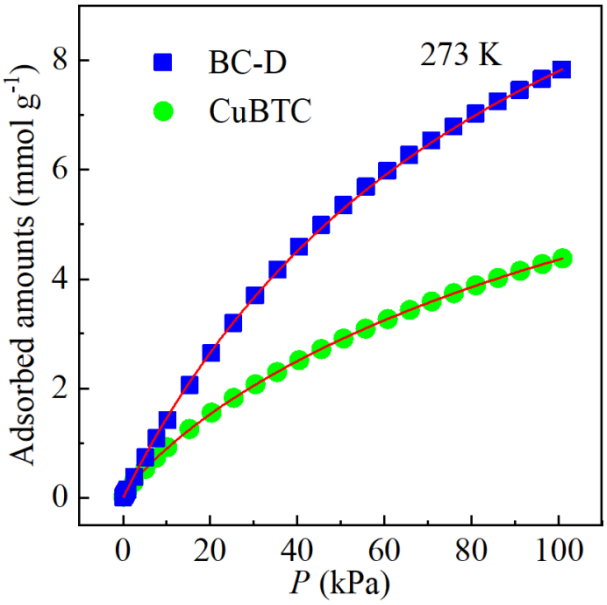

Fig. S13 CO_2 adsorption isotherms of CuBTC and BC-CuBTC-D-160 at 273 K. The isotherms were fitted by lines from single-site Langmuir-Freundlich equation.

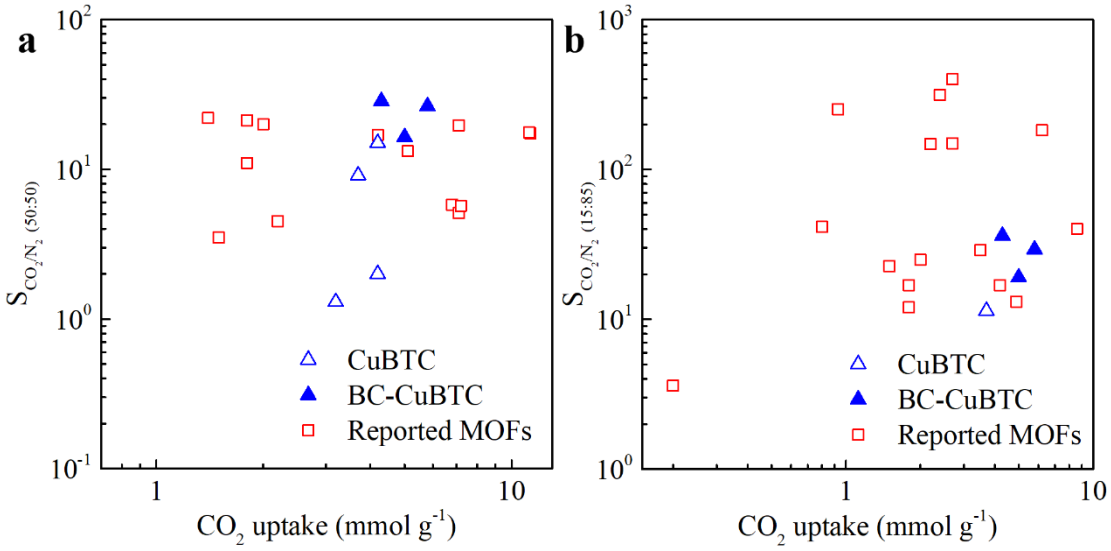

Fig. S14 Comparison of CuBTC and BC-CuBTC with other MOF materials in carbon capture for (a) CO_2/N_2 (50:50) and (b) CO_2/N_2 (15:85) mixtures.

Table S1 Peak intensity ratios for CuBTC and BC-CuBTC from PXRD patterns.

Samples	{220}/{222}	{400}/{222}
CuBTC	0.60	0.66
BC-CuBTC-M	0.20	0.32
BC-CuBTC-E	0.32	0.25
BC-CuBTC-D	0.38	0.25

Table S2 Porous properties of CuBTC and BC-CuBTC.

Samples	BET surface area (m^2 g^{-1})	Pore area (m^2 g^{-1})		Pore volume (mL g^{-1})	
		Micropore	Mesopore	Micropore	Mesopore
CuBTC[4]	1329	1282	47.8	0.49	0.010
BC-CuBTC-M	1813	1745	68.8	0.71	0.080
BC-CuBTC-E	1811	1734	76.7	0.71	0.022
BC-CuBTC-D	1843	1743	99.6	0.73	0.033
BC-CuBTC-D-160	1270	1065	205	0.50	0.100

Table S3 Gas areas and proportions of the air in container before and after self-conversion.

	A_{CO_2}	$A_{N_2+O_2}$	$A_{CO_2}/A_{N_2+O_2+CO_2}$(%)
Air	940.69	3101649	0.030
BC-CuBTC-M	4446.92	4629069	0.096
BC-CuBTC-E	5015.28	4978704	0.101
BC-CuBTC-D	4784.46	4931216	0.097

Table S4 Element content of CuBTC and BC-CuBTC from XPS.

Materials	C (%)	O (%)	Cu (%)
CuBTC	55.61	35.95	8.43
BC-CuBTC-M	54.86	36.22	8.92
BC-CuBTC-E	54.10	36.64	9.26
BC-CuBTC-D	55.19	35.99	8.82

Table S5 Chemical bond content of CuBTC and BC-CuBTC from C 1s XPS.

Materials	C-H C-C C=C (%)	C-COOH (%)	O-C=O (%)	CO_3^{2-} (%)
CuBTC	60.94	15.89	23.19	0
BC-CuBTC-M	53.10	25.74	15.19	5.97
BC-CuBTC-E	51.55	25.77	14.47	8.21
BC-CuBTC-D	53.71	24.66	14.61	7.02

Table S6 $Cu_2(OH)_2CO_3$ content of CuBTC and BC-CuBTC.

Materials	$Cu_2(OH)_2CO_3$ (wt %)
CuBTC	0
BC-CuBTC-M	2.34
BC-CuBTC-E	3.91
BC-CuBTC-D	1.88

Table S7 Comparison of CuBTC and BC-CuBTC with other MOF materials reported in previous studies for carbon capture at 100 kPa. *Henry's law.

Materials	S_{BET} (m^2 g^{-1})	Temp (K)	Capacity (mmol g^{-1})		IAST selectivity	Ref
			CO_2	N_2		
CuBTC	1482	295	3.5	0.3		5
CuBTC	1272	298	4.1			6
CuBTC/MoS_2	1639	298	4.6			6
CuBTC	1492	298	4.2	0.4	15.0 (50/50)	7
CuBTC	1448	298	4.0			8
CuBTC/HCM	516	298	2.8	0.3		8
CuBTC	933	298	2.8			9
CuBTC/GO	837	298	3.4			9
CuBTC	1781	298	4.1			10
CuBTC	1080	298	3.2	0.37	1.3 (50:50)	11
CuBTC/PEI	886	298	4.2	0.45	2.0 (50:50)	11
CuBTC/AC-2	1381	298	5.4	0.2		12
CuBTC/GO	1367	298	12.5	2.2		13
Mg-MOF-74	1640	296	6.2	0.2	182.1 (15/85)	14-16
MOF-177		296	0.2	0.2	3.6 (15/85)	15, 16
USTA-16	628	296	2.4	0.04	314.7 (15/85)	16, 17
rth-MOF-7	1900	298	3.5		25.0 (10/90)	17-19

SiFSIX-2-Cu	3140	298	1.8	0.2	13.7 (10/90)	19, 20
ZIF-78		296	0.8	0.1	41.4 (15/85)	19, 21
MIL-47		298	7.1	0.4	19.7 (50:50)	22
IRMOF-1		298	6.8	1.3	5.8 (50:50)	22
IRMOF-11		298	11.3	0.8	17.4 (50:50)	22
IRMOF-12		298	7.1	1.4	5.1 (50:50)	22
IRMOF-13		298	11.2	0.8	17.6 (50:50)	22
IRMOF-14		298	7.2	1.6	5.7 (50:50)	22
$Zn_4O(BDC)_3$	1200-1900	298	5.1	3.5	13.2 (50:50)	23
$[Cu_2(BPDC)_2]$	1280	298	8.6	0.6	40.2 (15:85)	23
NTU-101-Cu	2017	273	4.5	0.3		24
IITKGP-11	253	295	2.7	0.2	149 (15:85)	25
MIL-101(Cr)	3150	298	2.0	0.2	25 (15:85) 20 (50:50)	26
MIL-101(Cr)	3355	298	1.8	0.2	12 (15:85) 11 (50:50)	26
MOF-505	1076	298	3.5	0.3	29 (15:85)	27
IITKGP-5	366	295	2.2	0.2	148 (15:85)	28
NENU-520	387	298	2.7	0.01	400 (15:85)	29
ZIF-300	420	298	1.4	0.1	22 (50:50)*	30
MOF-508b		303	2.2	1.1	4.5 (50:50)	31
ROD-6	345	298	1.8	0.17	16.9 (15:85)	32

					21.2 (50:50)	
ROD-7	1189	298	1.5	0.1	22.7 (15:85) 3.5 (50:50)	32
NU-1000	2320	293	1.8	0.2	7.9 (10:90)	33
$[Zn(L)\cdot H_2O]\cdot DMA$	185	273	0.93	0.3	252.0 (15:85)	34
LCU-105	835	298	4.9 (0.75 bar)	0.5 (0.75 bar)	13.1 (15:85)	35
LCU-106	620	298	4.2 (0.75 bar)	0.3 (0.75 bar)	16.9 (15:85)	35
CuBTC	1329	298	3.7	0.5	11.4 (15:85) 9.1 (50:50)	4 This work
BC-CuBTC-M	1813	298	5.0	0.3	19.0 (15:85) 16.4 (50:50)	This work
BC-CuBTC-E	1811	298	5.8	0.2	29.2 (15:85) 26.4 (50:50)	This work
BC-CuBTC-D	1843	298	4.3	0.1	36.1 (15:85) 28.5 (50:50)	This work

Table S8 Parameters in the single-site Langmuir-Freundlich equation fitted to adsorption of pure CO_2 and N_2 at 273 and 298 K.

Materials	gas	a	b	n
CuBTC	CO_2 (273 K)	11.57832	0.01164	0.8573
	CO_2	14.55524	0.00466	0.93023
	N_2	1.89849	0.0017	1.136
BC-CuBTC-M	CO_2	21.13285	0.00271	1.03485
	N_2	0.77935	0.00317	1.15137
BC-CuBTC-E	CO_2	22.42368	0.00287	1.0417
	N_2	0.9521	0.002	1.10076
BC-CuBTC-D	CO_2 (273 K)	15.32211	0.01061	0.99527
	CO_2	17.49284	0.00348	0.99488
	N_2	0.33777	0.00397	1.15364

References

1. S.-C. Qi, X.-Y. Qian, Q.-X. He, K.-J. Miao, Y. Jiang, P. Tan, X.-Q. Liu and L.-B. Sun, *Angew. Chem. Int. Ed.*, 2019, **58**, 10104–10109.
2. A. A. Talin, A. Centrone, A. C. Ford, M. E. Foster, V. Stavila, P. Haney, R. A. Kinney, V. Szalai, F. E. Gabaly, H. P. Yoon, F. Léonard and M. D. Allendorf, *Science*, 2014, **343**, 66–69.
3. A. S. Hall, A. Kondo, K. Maeda and T. E. Mallouk, *J. Am. Chem. Soc.*, 2013, **135**, 16276–16279.
4. M. Jia, L. Mai, Z. Li and W. Li, 2020, **12**, 14171–14179.
5. P. Chowdhury, C. Bikkin, D. Meister, F. Dreisbach and S. Gumma, *Microporous Mesoporous Mater.*, 2009, **117**, 406–403.
6. X. Mu, S. Liu, Y. Chen, U. Kei Cheang, M. W. George and T. Wu, *Ind. Eng. Chem. Res.*, 2020, **59**, 5808–5817.
7. A. O. Yazaydin, A. I. Benin, S. A. Faheem, P. Jakubczak, J. J. Low, R. R. Willis and R. Q. Snurr, *Chem. Mater.*, 2009, **21**, 1425–1430.
8. D. Qian, C. Lei, G.-P. Hao, W.-C. Li and A.-H. Lu, *ACS Appl. Mater. Interfaces*, 2012, **4**, 6125–6132.
9. Z. J. Bian, J. Xu, S. P. Zhang, X. M. Zhu, H. L. Liu and J. Hu. *Langmuir*, 2015, **31**, 7410–7417.
10. A. R. Millward and O. M. Yaghi, *J. Am. Chem. Soc.*, 2005, **127**, 17998–17999.
11. A. Aarti, S. Bhadauria, A. Nanoti, S. Dasgupta, S. Divekar, P. Gupta and R. Chauhan, *RSC Adv.*, 2016, **6**, 93003–93009.

12. H. J. Park and, M. P. Suh, *Chem. Sci.*, 2013, **4**, 685–690.

13. A. Policicchio, Y. Zhao, Q. Zhong, R. G. Agostino and T. J. Bandosz, *ACS Appl. Mater. Interfaces*, 2014, **6**, 101−108.

14. P. D. C. Dietzel, V. Besikiotis and R. Blom, *J. Mater. Chem.*, 2009, **19**, 7362–7370.

15. J. A. Mason, K. Sumida, Z. R. Herm, R. Krishna and J. R. Long, *Energy Environ. Sci.*, 2011, **4**, 3030–3040.

16. S. Xiang, Y. He, Z. Zhang, H. Wu, W. Zhou, R. Krishna, B. Chen, *Nat. Commun.*, 2012, **3**, 954.

17. Y. Belmabkhout, V. Guillerm, M. Eddaoudi and Y. Belmabkhout, *Chem. Eng. J.*, 2016, **296**, 386–397.

18. R. Luebke, J. F. Eubank, A. J. Cairns, Y. Belmabkhout, L. Wojtas and M. Eddaoudi, *Chem. Commun.*, 2012, **48**, 1455–1457.

19. M. Oschatz and M. Antonietti, *Energy Environ. Sci.*, 2018, **11**, 57–70.

20. P. Nugent, Y. Belmabkhout, S. D. Burd, A. J. Cairns, R. Luebke, K. Forrest, T. Pham, S. Ma, B. Space, L. Wojtas, M. Eddaoudi and M. J. Zaworotko, *Nature*, 2013, **495**, 80–84.

21. R. Banerjee, H. Furukawa, D. Britt, C. Knobler, M. O'Keeffe and O. M. Yaghi, *J. Am. Chem. Soc.*, 2009, **131**, 3875–3877.

22. B. Liu, B. Smit, *Langmuir*, 2009, **25**, 5918–5926.

23. C. He, C. Hou, Y. M. Wang, X. Y. Gong, H. L. Jiang, Y. B. Sun, K. Liu and X. Q. Cao, *CrystEngComm*, 2020, **22**, 3378–3384.

24. X.-J. Wang, P.-Z. Li, L. Liu, Q. Zhang, P. Borah, J. D. Wong, X. X. Chan, G. Rakesh, Y. Lia and Y. Zhao, *Chem. Commun.*, 2012, **48**, 10286–10288.

25. A. Pal, S. Chand, D. G. Madden, D. Franz, L. Ritter, A. Johnson, B. Space, T. Curtin and M. C. Das, *Inorg. Chem.*, 2019, **5**, 11553–11560.

26. Y. Lin, H. Lin, H. Wang, Y. Suo, B. Li, C. Kong and L. Chen, *J. Mater. Chem. A*, 2014, **2**, 14658–14665.

27. Y. Chen, H. Wu, Q. Xiao, D. Lv, F. Li, Z. Li and Q. Xia, *CrystEngComm*, 2019, **21**, 165–171.

28. A. Pal, S. Chand, S. M. Elahi and M. C. Das, *Dalton Trans.*, 2017, **46**, 15280–15286.

29. S. Bao, R. Krishna, Y. He, J. Qin, Z. Su, S. Li, W. Xie, D. Du, W. He, S. Zhang and Y. Lan, *J. Mater. Chem. A*, 2015, **3**, 7361–7367.

30. N. T. T. Nguyen, H. Furukawa, F. Gándara, H. T. Nguyen, K. E. Cordova and O. M. Yaghi, *Angew. Chem. Int. Ed.*, 2014, **53**, 10645–10648.

31. L. Bastin, P. S. Barcia, E. J. Hurtado, J. A. C. Silva, A. E. Rodrigues and B. Chen, *J. Phys. Chem. C*, 2008, **112**, 1575–1581.

32. R.-J. Li, M. Li, X.-P. Zhou, D. Li and M. O'Keeffe, *Chem. Commun.*, 2014, **50**, 4047–4049.

33. P. Deria, J. E. Mondloch, E. Tylianakis, P. Ghosh, W. Bury, R. Q. Snurr, J. T. Hupp and O. K. Farha, *J. Am. Chem. Soc.*, 2013, **135**, 16801–16804.

34. X. Lv, L. Li, S. Tang, C. Wang and X. Zhao, *Chem. Commun.*, 2014, **50**, 6886–6889.

35. H. Y. Ma, Y. Z. Zhang, H. Yan, W. J. Zhang, Y. W. Li, S. N. Wang, D. C. Li, J. M. Dou and J. R. Li, *Dalton Trans.*, 2019, **48**, 13541–13545.